



# Tetramethylpyrazine mitigates lipopolysaccharide-induced acute lung injury by inhibiting the HMGB1/TLR4/NF- $\kappa$ B signaling pathway in mice

Xu He<sup>1,2</sup>, Guo-Feng Chen<sup>1,2</sup>, Wei-Ting Tao<sup>3</sup>, Xiao-Jia Huang<sup>2</sup>, Ye Lin<sup>2</sup>, Jing Sun<sup>2</sup>, Yan Li<sup>2</sup>

<sup>1</sup>School of Pharmacy & School of Biological and Food Engineering, Changzhou University, Changzhou, China; <sup>2</sup>School of Medical and Health Engineering, Changzhou University, Changzhou, China; <sup>3</sup>School of Basic Medicine, Bengbu Medical University, Bengbu, China

**Contributions:** (I) Conception and design: X He, Y Li; (II) Administrative support: None; (III) Provision of study materials or patients: XJ Huang, Y Lin, J Sun; (IV) Collection and assembly of data: X He, GF Chen, WT Tao; (V) Data analysis and interpretation: X He, Y Li; (VI) Manuscript writing: All authors; (VII) Final approval of manuscript: All authors.

**Correspondence to:** Yan Li, MD in Pathophysiology. School of Medical and Health Engineering, Changzhou University, No. 1 Gehu Middle Road, Hutang Town, Wujin District, Changzhou 213164, China. Email: liyan37@mail3.sysu.edu.cn.

**Background:** Tetramethylpyrazine (TMP) possesses anti-inflammatory and antioxidant properties and plays a crucial role in mitigating acute lung injury (ALI). However, the specific underlying mechanisms remain elusive. High mobility group box 1 (HMGB1), a pro-inflammatory factor, can bind to Toll-like receptor 4 (TLR4), activating downstream signaling pathways, which in turn activate nuclear factor kappa-B (NF- $\kappa$ B). This study aims to explore the preventive effects of TMP on lipopolysaccharide (LPS)-induced ALI and its influence on the HMGB1/TLR4/NF- $\kappa$ B signaling pathway.

**Methods:** C57BL/6 mice were randomly divided into a control group (CON group), a model group (LPS group), a heparin (Hep) group, and a TMP group. In the model group, mice received an initial intraperitoneal injection of LPS followed by a second airway injection three hours later to induce ALI. In the TMP group, LPS was administered 30 minutes before the first intraperitoneal injection and followed by intratracheal atomization of LPS. TMP was injected intraperitoneally 30 minutes after the second LPS administration. The Hep group received heparin at 200 IU/kg following the same schedule as the TMP group. Peripheral capillary oxygen saturation (SpO<sub>2</sub>) was measured 24 hours after the initial intraperitoneal injection. Lung tissues were harvested for wet to dry weight ratio (W/D) calculation and pathological assessment via hematoxylin and eosin (HE) staining. Western blot analysis was performed to evaluate the protein levels of HMGB1, TLR4, and NF- $\kappa$ B p65 in lung tissues, along with the assessment of leukocyte content and protein concentration in bronchoalveolar lavage fluid (BALF).

**Results:** Compared to the control group, the model group showed reduced SpO<sub>2</sub> levels, increased inflammatory indicators, and elevated expression levels of HMGB1, TLR4, and phosphorylated p65 (p-p65) proteins. TMP treatment led to a decrease in the W/D, reduced alveolar exudation, improved alveolar structure, and decreased total white blood cell count and protein concentration in BALF. Notably, the protein levels of HMGB1, TLR4, and p-p65 were significantly reduced in the TMP and Hep groups, while there were no significant differences in p65 expression among the groups.

**Conclusions:** TMP can alleviate LPS-induced ALI in mice by reducing lung inflammatory response through inhibiting the HMGB1/TLR4/NF- $\kappa$ B pathway.

**Keywords:** Tetramethylpyrazine (TMP); acute lung injury (ALI); HMGB1/TLR4/NF- $\kappa$ B signaling pathway

Submitted Sep 20, 2024. Accepted for publication Jan 17, 2025. Published online Mar 26, 2025.

doi: 10.21037/jtd-24-1561

View this article at: <https://dx.doi.org/10.21037/jtd-24-1561>

## Introduction

Acute lung injury (ALI) is a life-threatening condition characterized by severe inflammation and impaired lung function. It is often triggered by a variety of factors, including infection, sepsis, trauma, and inhalation of toxic substances. The pathogenesis of ALI involves the infiltration of inflammatory cells into the lungs, leading to the release of pro-inflammatory mediators that damage alveolar epithelial cells and pulmonary microvascular endothelial cells (1,2). This damage can result in increased capillary permeability, fluid leakage, and impaired gas exchange.

One key mediator of inflammation in ALI is high mobility group box 1 (HMGB1), a nuclear protein that can be released into the extracellular space under pathological conditions. HMGB1 binds to Toll-like receptor 4 (TLR4), activating downstream signaling pathways that promote

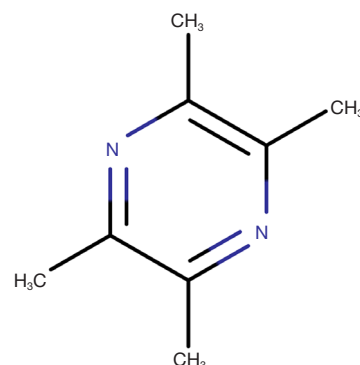


**Figure 1** The chemical structure of tetramethylpyrazine.

inflammation (3), including the nuclear factor kappa-B (NF- $\kappa$ B) pathway, which is a key signaling pathway in the treatment of ALI (4,5).

Tetramethylpyrazine (TMP) is a bioactive compound derived from the rhizome of *Ligusticum chuanxiong*, a traditional Chinese medicinal herb (6). Previous studies have demonstrated the anti-inflammatory properties of TMP and its potential benefits in various inflammatory diseases (7,8). However, the specific mechanisms underlying its protective effects against ALI remain unclear.

This study aimed to investigate the role of TMP in mitigating LPS-induced ALI and to explore its potential mechanisms of action. We hypothesized that TMP could attenuate ALI by inhibiting the HMGB1/TLR4/NF- $\kappa$ B signaling pathway. We present this article in accordance with the ARRIVE reporting checklist (available at <https://jtd.amegroups.com/article/view/10.21037/jtd-24-1561/rc>).

## Methods

### Materials

TMP was purchased from the First Affiliated Hospital of Bengbu Medical University. The molecular formula of TMP was determined as  $C_8H_{12}N_2$ , and the molecular weight of TMP was analyzed as 136.194. The chemical structure of TMP is presented in *Figure 1*. Heparin sodium was purchased from BioFroxx; LSP (L2630) was purchased from Sigma. Goat anti-rabbit/mouse II antibody, HMGB1 (Cat# 10829-1-AP, RRID: AB\_2232989), NF- $\kappa$ B p65 (Cat# CL488-10745, RRID: AB\_2918995), Phospho-NF- $\kappa$ B p65 (Cat# 82335-1-RR, RRID: AB\_3083091), and Beta Actin (Cat# 81115-1-RR, RRID: AB\_2923704) antibodies were purchased from Wuhan Mitaka Biotechnology Co.,

### Highlight box

#### Key findings

- Our study reveals that tetramethylpyrazine (TMP) effectively mitigates lipopolysaccharide (LPS)-induced acute lung injury (ALI) in mice by inhibiting the HMGB1/TLR4/NF- $\kappa$ B signaling pathway, a critical mediator of inflammatory responses.
- TMP administration led to improved oxygen saturation, reduced lung edema, and decreased inflammatory cell infiltration in the lungs, indicating a potent anti-inflammatory effect.
- The treatment with TMP resulted in downregulation of key inflammatory markers, suggesting its potential as a therapeutic agent in managing ALI.

#### What is known and what is new?

- It is known that ALI is a severe condition characterized by an inflammatory response in the lungs, often triggered by infections or sepsis. The HMGB1/TLR4/NF- $\kappa$ B pathway is well-recognized for its role in promoting inflammation in ALI.
- The novel application of TMP in inhibiting the HMGB1/TLR4/NF- $\kappa$ B axis in an LPS-induced ALI model highlights a specific mechanism of action that has not been previously explored, contributing new knowledge to the field.

#### What is the implication, and what should change now?

- The findings imply that TMP could be a viable therapeutic option for ALI, particularly in managing the inflammatory cascade triggered by LPS.
- Integrating TMP into ALI treatment could provide a novel therapeutic direction, and future clinical trials should focus on evaluating the efficacy and safety of TMP in human subjects, potentially leading to a new treatment strategy for ALI and other inflammatory lung diseases.

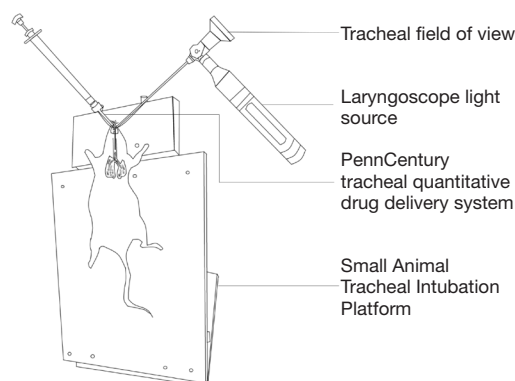


**Figure 2** Intratracheal aerosol dosing in mice.

Ltd. TLR4 (Cat#ab217274, RRID: AB\_2891074) was purchased from abcam. Radio immunoprecipitation assay (RIPA) lysis buffer (strong), protease phosphatase inhibitor mixture, and red blood cell lysis buffer were purchased from Beyotime. The bicinchoninic acid assay (BCA) detection kit was purchased from Formax Biotechnology. Electrochemiluminescence (ECL) chemiluminescence chromogenic solution was purchased from Shanghai Qinxian Technology Instrument Co., Ltd.

### Experimental animal

Male C57BL/6 mice of specific pathogen free (SPF)-grade (Institute for Cancer Research) ICR strain, aged between 6 and 7 weeks and weighing  $22 \pm 2$  g, were obtained from Changzhou Cavins Experimental Animal Co., Ltd. under the experimental animal production license number SCXK (Su) 2021-0013. The mice were housed in a barrier environment at SPF level. The environment was maintained with a 12-hour light/dark cycle, a temperature of  $24 \pm 2$  °C, and a relative humidity of  $(55 \pm 5)\%$ . The mice had free access to food and water. All animal experiments were performed under a project license (No. 20240308049) granted by the Biomedical Research Ethics Committee of Changzhou University, in compliance with Chinese national guidelines for the care and use of animals.

### Experimental protocols

#### Animal grouping and modeling

Sixty C57BL/6 mice were randomly divided into four groups: control (CON) group, model (LPS) group, Hep group, and TMP group, with 15 mice in each group. The

ALI mouse model was prepared as follows: Prior to the experiment, LPS was prepared in solutions of 0.5 and 4 mg/mL. Each mouse was initially given an intraperitoneal injection of LPS at a dose of 2 mg/kg. For the second injection, a small animal anesthesia machine (universal/isoflurane/PourFill-0-4L) was used to anesthetize the mouse. Then, the mouse was placed in the operating position. A laryngoscope light source was positioned at the mouse's mouth to expose the tracheal field of view. The airway was nebulized with LPS (8 mg/kg) using a Yuyan airway nebulizer. The animals were euthanized 24 hours after intraperitoneal injection (as shown in *Figure 2* and *Figure 3A*). Immediately after atomization, the animal was placed upright and gently rotated left and right to establish the model. Mice in the control group received an intraperitoneal injection of the same volume of normal saline as the model group for the first injection, followed by airway atomization with an equivalent volume of normal saline for the second treatment. The TMP group was intraperitoneally injected with TMP at a dose of 80 mg/kg, while the Hep group received Hep at a dosage of 200 IU/kg. The injection time points for both treatment groups were set at 30 minutes before the first intraperitoneal injection of LPS and 30 minutes after the second airway atomization of LPS. Mice in the control and model groups were administered equal volumes of normal saline simultaneously with the Hep and TMP groups. Lung tissues and bronchoalveolar lavage fluid (BALF) were collected 24 hours after intraperitoneal injection of LPS. Samples were stored in a freezer at  $-80$  °C for further analysis. All experimental procedures were conducted blind to all groups. This included histological analysis, which was performed by a pathologist unaware of group assignments until after scoring was completed. A protocol was prepared before the study without registration.

#### Lung tissue wet to dry weight ratio detection

Absorb the moisture on the surface of the freshly excised lung tissue gently using absorbent paper and measure its wet weight accurately. Then, place the tissue in a  $65$  °C oven for 24 hours until a constant weight is attained. Determine the dry lung weight precisely and calculate the wet to dry weight ratio (W/D) using the appropriate formula.

#### BALF acquisition and testing

Anesthetize the mouse through intraperitoneal injection.

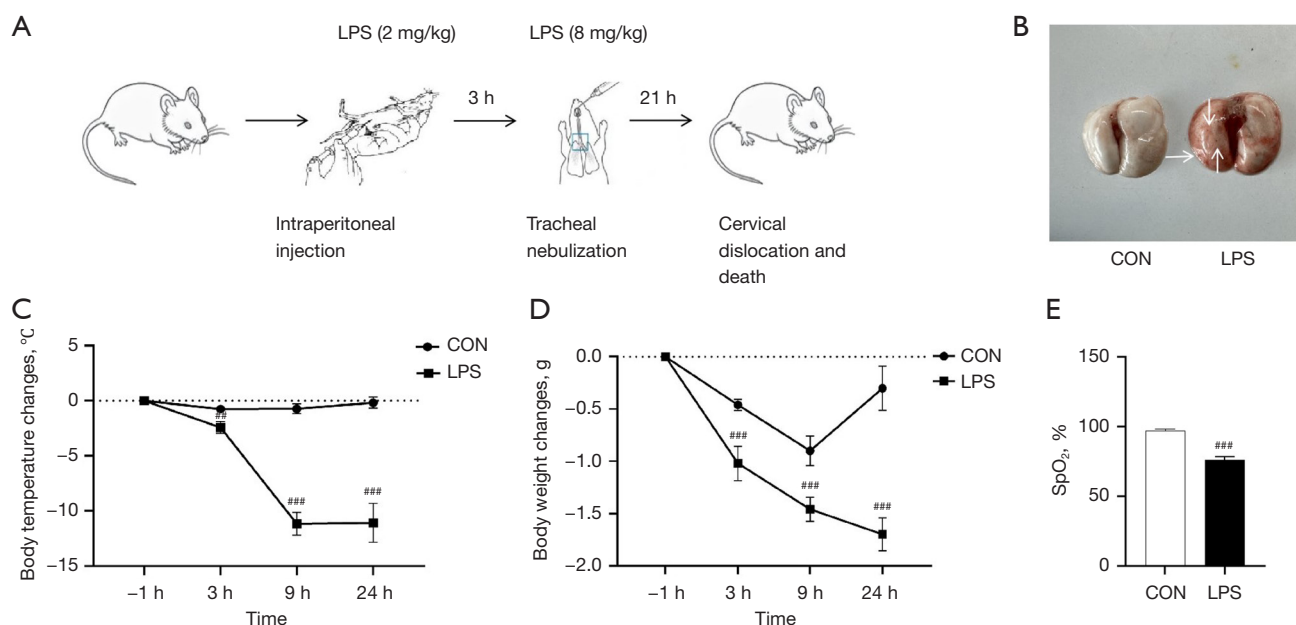


**Figure 3** LPS induced severe lung injury in mice. (A) LPS administration process. (B) The gross appearance of the lung was observed (white arrows: the inflammation/redness of lung tissues). (C,D) The changes in body temperature and weight of mice, respectively. (E) SpO<sub>2</sub>. Mean  $\pm$  SD,  $n=5$ .  $^{*}P<0.01$ ,  $^{***}P<0.001$  vs. CON group. CON, control; LPS, lipopolysaccharide; SD, standard deviation; SpO<sub>2</sub>, peripheral capillary oxygen saturation.

Open the chest cavity to expose the trachea and use hemostats to clamp five pieces of lung tissue while leaving the largest piece on the left intact. Rinse this tissue five times with pre-cooled phosphate-buffered saline (PBS) (0.4 mL), collect the alveolar lavage fluid, and then measure the protein concentration in the BALF using the BCA method. Additionally, the lungs of the mice were aspirated twice with pre-cold PBS (0.8 mL each time) and then centrifuged at 4 °C, 1,500 rpm for 10 minutes. After adding 500  $\mu$ L of red blood cell lysis buffer for 10 minutes, the samples were centrifuged again to get the pellet. The pellet was resuspended in 500  $\mu$ L cold PBS for white blood cell counting. A 40  $\mu$ L cell suspension was spread on a slide, air-dried, fixed with 70% ethanol for 10 minutes, and stained with modified Giemsa for 20 minutes. At least 200 cells were counted under a microscope to calculate their proportions among white blood cells. As this was a later-added experiment, we had to re-extract the lavage fluid to ensure its freshness for the differential count.

#### Body temperature and weight detection

Record the body temperature and weight of the animals at

four time points: one hour before the experiment and 3, 9, and 24 hours after the experiment. Animals with a body temperature exceeding 38 °C are excluded from the study. To analyze the data, calculate the difference between the body temperature and weight measurements at each post-experimental time point and the initial measurements taken before the experiment.

#### Hemodynamic measurements

Peripheral blood oxygen saturation was measured using the MouseOx Plus device (STARR Life Sciences Corp., 333 Allegheny Avenue, Suite 300, Oakmont, PA 15139). For each group of animals, measurements were taken 24 hours after the start of the experiment. Each animal was continuously monitored for at least 10 minutes. The continuous 10-minute data was intercepted, and peripheral capillary oxygen saturation (SpO<sub>2</sub>) values marked with a credible code were filtered to calculate the average value.

#### Histological analysis and lung injury scoring

Lung tissue was fixed in formalin for 24 hours, rinsed with

running water, dehydrated in ethanol, and embedded in paraffin. Sections of 6  $\mu\text{m}$  were prepared using a microtome and then baked in an oven at 65 °C for 3 hours. The sections were dehydrated with graded ethanol, stained with hematoxylin and eosin (HE), and sealed with neutral gum. Finally, the morphological changes of the lung tissue were observed under a light microscope. A pathologist blinded to the groups conducted histological analysis and lung injury scoring.

### ***Western immunoblotting analysis***

Take 50 mg of lung tissue and place it in a pre-cooled 1.5 mL round-bottom Eppendorf (EP) tube. Add two magnetic beads and 300  $\mu\text{L}$  of RIPA lysis buffer, and then lyse the tissue using an oscillating cell disruption system. Centrifuge the mixture at 12,000 r/min for 5 minutes and collect the supernatant. Mix the supernatant with sodium dodecyl sulfate-polyacrylamide gel electrophoresis (SDS-PAGE) protein loading buffer and heat at 99 °C for 10 minutes. Load 15  $\mu\text{g}$  of the sample per well. Run the gel at 90 V for 30 minutes and then switch to 130 V and run for an additional 60 minutes. Transfer the proteins to a membrane at 300 mA for 90 minutes. Block the membrane with 5% skim milk for 1 hour. Incubate the membrane with the primary antibody overnight at 4 °C. Prepare dilutions of antibodies for HMGB1 at a dilution factor of 1:1,500, TLR4 at 1:1,000, p65 at 1:2,000, p-p65 at 1:8,000, and  $\beta$ -actin at 1:20,000, in the appropriate proportions for experimental setup. Wash the membrane three times with Tris Buffered Saline with Tween-20 (TBST) for 3 minutes each. Incubate with the secondary antibody on a room temperature shaker for 1 hour, followed by two washes with TBST for 10 minutes each. Finally, develop the membrane using an ECL chemiluminescent agent and analyze the gray value using ChemiScope Analysis software.

### ***Statistical analysis***

Statistical analysis was performed using GraphPad Prism 9 software. All measurement data were evaluated for normality and presented as mean  $\pm$  standard deviation (SD). For comparisons between two groups under the conditions of normal distribution and homogeneity of variances, the *t*-test was applied. For comparisons involving multiple factors, two-way analysis of variance (ANOVA) was utilized.

Statistical significance was considered at a P value of  $<0.05$ .

## **Results**

### ***Effects of LPS on related physiological indicators in mice***

After LPS induction, the lungs of the mice in the model group showed prominent red congestion spots following the flushing of intravascular blood (*Figure 3B*). The weight and body temperature of the mice in the model group exhibited a significant downward trend (*Figure 3C, 3D*). Accompanying symptoms included loose stools, trembling, and a markedly reduced mobility. The diagnostic criterion for ALI in mice involves evaluating the degree of hypoxemia by measuring the ratio of arterial blood oxygen partial pressure ( $\text{PaO}_2$ ) to inhaled oxygen concentration percentage ( $\text{FiO}_2$ ) through arterial blood gas analysis (9,10). In this study, since the ALI animal model was constructed without ventilator support, we primarily chose a significant and sustained decrease in  $\text{SpO}_2$  rather than the  $\text{PaO}_2/\text{FiO}_2$  ratio to assess the degree of hypoxemia. The 10-minute continuous  $\text{SpO}_2$  measurements of mice in the model group were significantly lower than those of the control group, as shown in *Figure 3E*.

### ***Effects of TMP on lung histopathology in mice***

The results of HE staining indicated that the lung tissue structure of the mice in the control group was normal, with a clear tissue outline and no obvious abnormalities. In contrast, the mice in the LPS group had a significant presence of red blood cells in both the alveolar cavity and interstitium. Flaky blood lesions were visible to the naked eye, and the alveolar walls were thickened, accompanied by an expansion of the alveolar intervals. Additionally, inflammatory cell infiltration and lung tissue damage scores were significantly increased. In the TMP and Hep groups, red blood cell infiltration in the lung tissue was reduced, exudation in the alveolar cavity was diminished, and the alveolar walls were thinner compared to the LPS group. Moreover, inflammatory infiltration was lessened, the alveolar structure showed significant improvement, flaky blood lesions were markedly reduced, and the lung tissue damage score decreased significantly, as illustrated in *Figure 4*. Overall, HE staining demonstrated that TMP has a protective and ameliorative effect on the pathological lung damage induced by LPS.



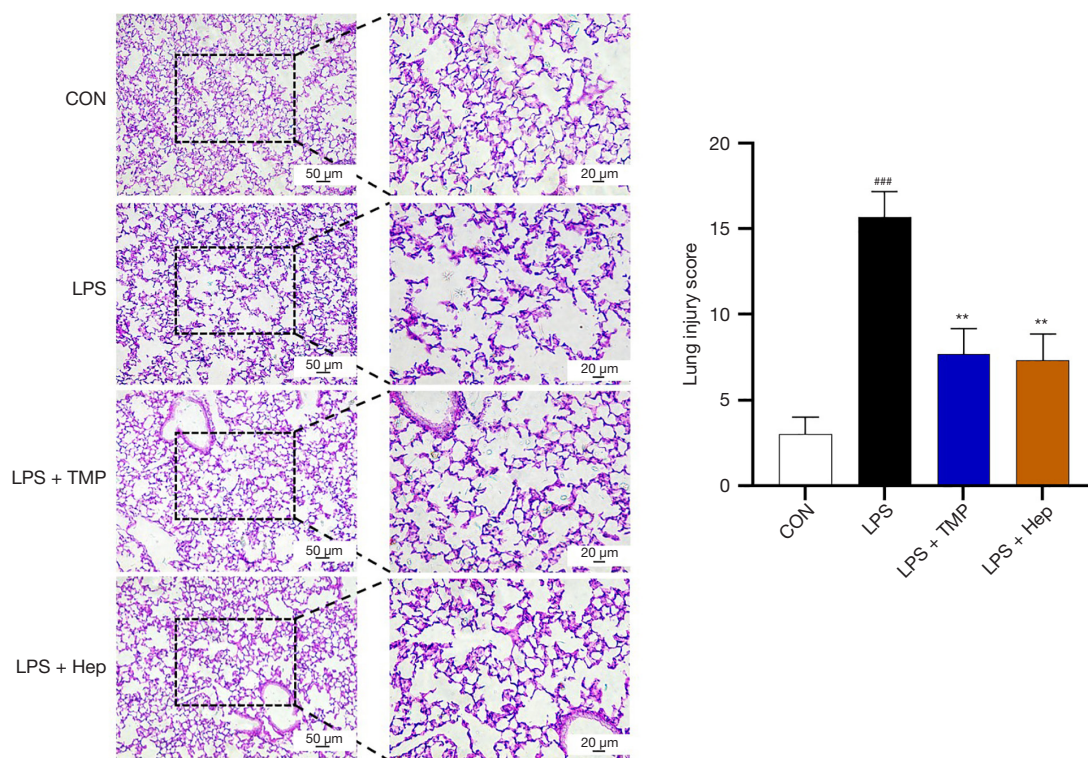


**Figure 4** The HE staining results and injury scores of mouse lung tissues. Mean  $\pm$  SD,  $n=3$ . ### $P<0.001$  vs. CON group; \*\* $P<0.01$  vs. LPS group. CON, control; HE, hematoxylin and eosin; Hep, heparin; LPS, lipopolysaccharide; SD, standard deviation; TMP, tetramethylpyrazine.

#### *Effects of TMP on lung inflammation and injury in ALI mice*

When inflammation or injury occurs in the lungs, vascular permeability increases, leading to edema, the leakage of plasma proteins into the alveolar fluid, and an elevation in the concentration of proteins in BALF. Additionally, inflammation results in an increased number of white blood cells in BALF. Compared to the control group, the W/D of the model group was significantly higher. In contrast, the W/D of the TMP and Hep groups were significantly lower than that of the model group, as illustrated in *Figure 5A*.

The protein concentration in BALF was measured using the BCA method. It was revealed that, relative to the control group, the protein concentration in BALF of mice in the model group was significantly elevated. Furthermore, the protein concentration in the BALF of the TMP group was significantly reduced compared to the model group, with a trend that was in line with the results of the positive control group, as depicted in *Figure 5B*.

Compared to the control group, the LPS group displayed a significant elevation in BALF white blood cell counts, with pronounced increases in neutrophils, lymphocytes, and eosinophils. Conversely, TMP and Hep treatments mitigated this increase in BALF leukocytes, reducing the proportion of all types except macrophages (*Figure 5C, 5D*).

#### *TMP inhibits the activation of HMGB1/TLR4/NF- $\kappa$ B p65 pathway in LPS-induced ALI mice*

Based on the high expression of related proteins in the model group of mice, we observed that LPS effectively activated the HMGB1/TLR4 inflammatory pathway. Following treatment with TMP and Hep, the expression levels of HMGB1 and TLR4 proteins were significantly reduced, suggesting that TMP can inhibit the activation of inflammatory pathways induced by LPS. Additionally, we investigated the activation of NF- $\kappa$ B p65 within the downstream pathway. The levels of p-p65 were significantly up-regulated in the model group (*Figure 6*), confirming that LPS successfully activated the downstream pathway.

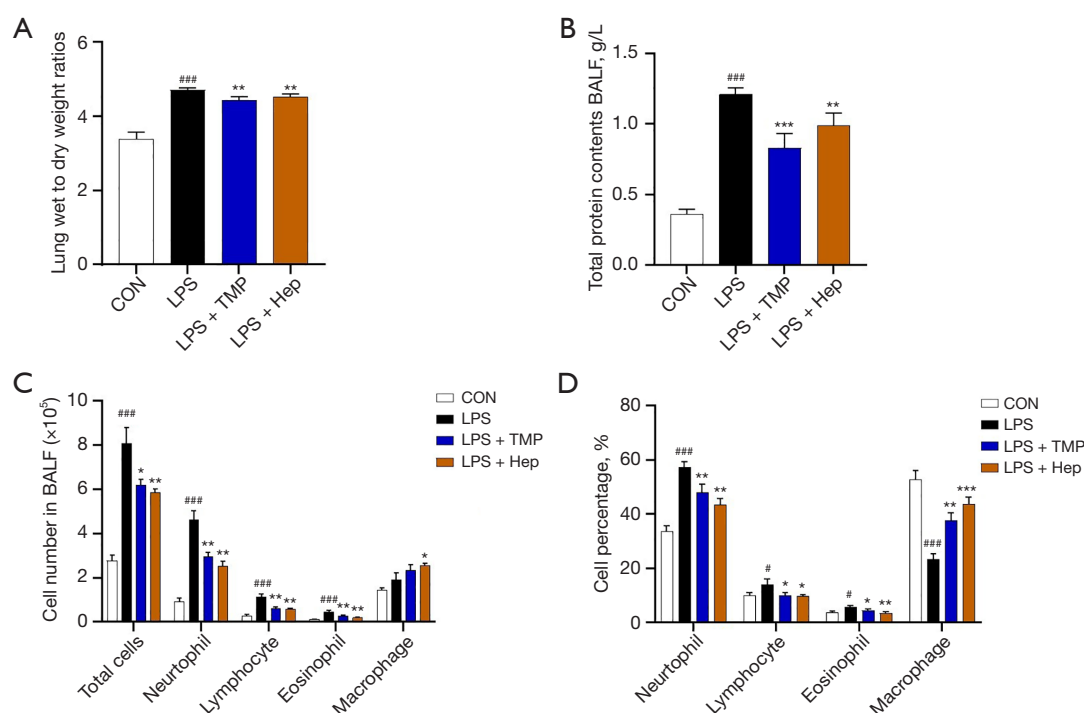


**Figure 5** Effects of TMP on protein concentration and leukocyte count and classification in BALF of mice. (A) Effect of TMP on lung wet-to-dry weight ratio in ALI mice. Mean  $\pm$  SD,  $n=4$ . (B) BCA was used to measure the protein concentration in BALF. Mean  $\pm$  SD,  $n=5$ . (C) Total white blood cell counts and differential count in BALF. (D) The proportion of various types of white blood cells in the total white blood cell count. Mean  $\pm$  SD,  $n=3$ . <sup>#</sup> $P<0.05$ , <sup>###</sup> $P<0.001$  vs. CON group; <sup>\*</sup> $P<0.05$ , <sup>\*\*</sup> $P<0.01$ , <sup>\*\*\*</sup> $P<0.001$  vs. LPS group. ALI, acute lung injury; BALF, bronchoalveolar lavage fluid; BCA, bicinchoninic acid assay; CON, control; Hep, heparin; LPS, lipopolysaccharide; SD, standard deviation; TMP, tetramethylpyrazine.

Conversely, TMP was found to down-regulate the protein expression of p-p65, indicating that it exerts an inhibitory effect on the HMGB1/TLR4/NF- $\kappa$ B inflammatory pathway.

## Discussion

ALI is primarily characterized by damage to alveolar epithelial cells and microvascular endothelial cells, accompanied by diffuse edema in the lung interstitium and alveoli, ultimately leading to acute hypoxic respiratory insufficiency. Infectious agents are the most common cause of ALI. Lipopolysaccharide (LPS), the main component of the cell wall of Gram-negative bacteria, can activate neutrophils, alveolar macrophages (AM), and other cells, resulting in the release of a significant amount of pro-inflammatory factors that trigger a systemic inflammatory response. This response is a leading cause of acute respiratory failure and is considered one of the

common predisposing factors (11-13). In the Shwartzman phenomenon, the initial injection of endotoxin can lead to the closure of the mononuclear phagocyte system; however, a subsequent injection of endotoxin fails to effectively clear the endotoxin due to the inhibition of mononuclear phagocyte system function, leading to local or systemic pathological reactions. In this experiment, the “double-hit” model using LPS is employed to induce an ALI mouse model. The initial hit activates the mouse’s immune system, while the subsequent hit causes more prominent lung damage, thereby more closely mimicking clinical ALI. The modeling approach utilized in this study involves intra-airway atomization for drug administration (Figure 2). Compared with inhalation drug delivery via an atomizer box, this method ensures that each mouse achieves the desired drug levels to the greatest extent possible. Additionally, compared to traditional surgical techniques that require tracheal exposure for drug administration, this non-invasive method leverages atomization technology to

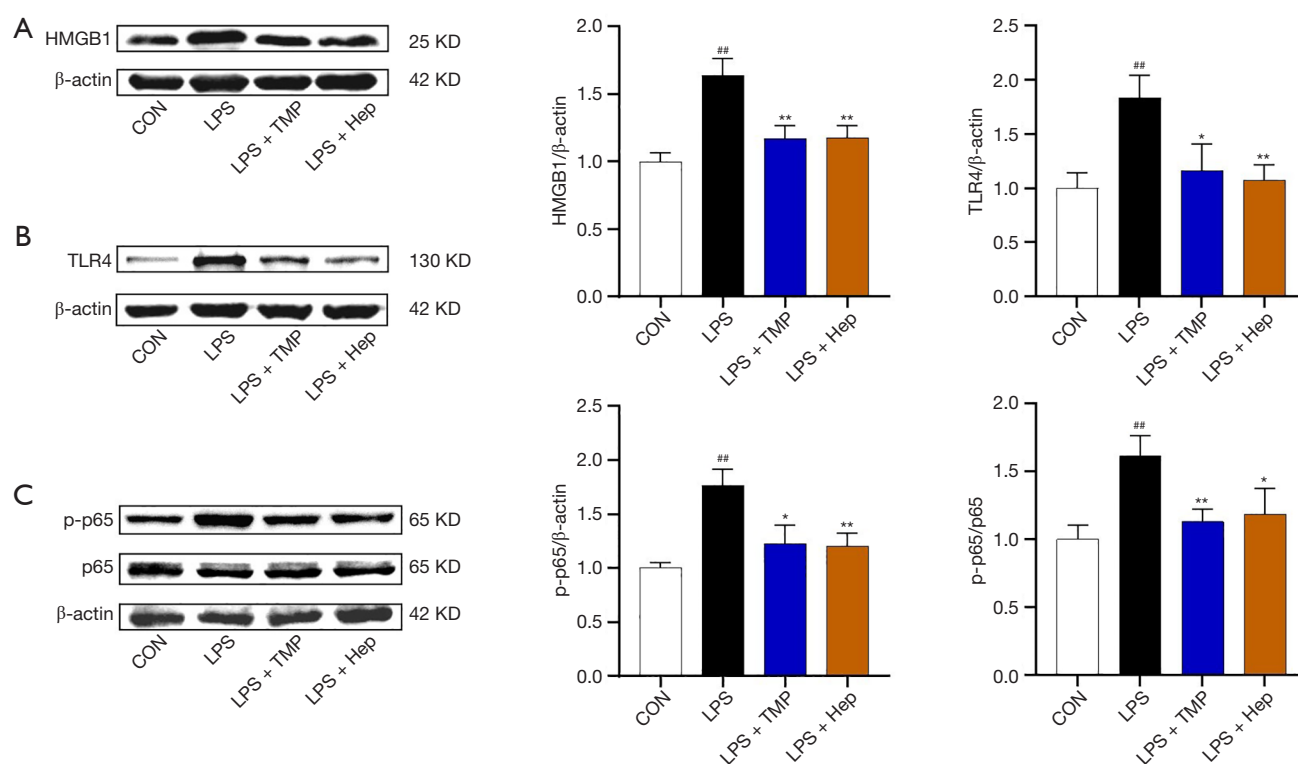


**Figure 6** Effect of TMP pre-protection on the protein levels of HMGB1, TLR4, p65 and p-p65 in lung tissue of the mice with LPS-induced ALI. (A,B) The protein levels of HMGB1 and TLR4 were determined by Western blot. (C) The protein levels of p65 and p-p65 were determined by Western blot. Mean  $\pm$  SD,  $n=3$ . <sup>##</sup> $P<0.01$  vs. CON group; <sup>\*</sup> $P<0.05$ , <sup>\*\*</sup> $P<0.01$  vs. LPS group. ALI, acute lung injury; CON, control; Hep, heparin; HMGB1, high mobility group box 1; LPS, lipopolysaccharide; p-p65, phosphorylated p65; SD, standard deviation; TLR4, Toll-like receptor 4; TMP, tetramethylpyrazine.

uniformly distribute the drug throughout the lungs, thereby reducing the risk of pulmonary complications associated with choking on the medication. These advantages enhance the feasibility of conducting research based on this model.

TMP is an alkaloid extracted from the rhizome of *Ligusticum wallichii* and has multiple bioactivities (14). Previous study has demonstrated its anti-inflammatory and immunomodulatory properties, suggesting its potential therapeutic applications (15).

Heparin sodium is a well-established anticoagulant that has also been shown to possess anti-inflammatory properties (16). Heparin can inhibit the release of inflammatory mediators and improve microcirculation (17), potentially beneficial for conditions like ALI. Additionally, heparin can reduce fibrin deposition in the lungs, which may enhance oxygenation (18).

In this study, we used heparin as a positive control to compare its effects with TMP. Previous research from our group has shown that varying doses of TMP can improve

ALI, with a middle dose of 80 mg/kg demonstrating the most significant efficacy (19,20). Therefore, we selected this dosage for our study to investigate the protective effects of TMP against LPS-induced ALI. The resulting human equivalent dose of TMP (9 mg/kg), based on the equivalent dose ratio between mice and humans (9.1:1), differs from established clinical dosages for cardiovascular applications. This difference might arise from variations in drug bioavailability and the distinct pathophysiological mechanisms involved in ALI compared to cardiovascular diseases.

HMGB1 is a multifunctional nuclear protein with various biological roles both inside and outside of cells. Under physiological conditions, HMGB1 is primarily localized in the nucleus. However, in pathological circumstances, it is released into the extracellular space. There are two principal sources of extracellular HMGB1. Firstly, it can be actively secreted by monocytes, macrophages, tissue cells, neutrophils, and dendritic cells after stimulation and



activation. Secondly, HMGB1 is passively released into the extracellular environment when cells are damaged, lysed, or die due to biological factors (21). Once released, HMGB1 functions as a late inflammatory mediator, activating downstream signaling pathways and promoting the onset of inflammatory responses by binding to various receptors, including TLR2, TLR4, and advanced glycation end product receptor (AGER) (22). The protein concentration in BALF and the total number of white blood cells in the model group were significantly increased, indicating that LPS caused damage to the pulmonary vascular barrier. This led to the leakage of intravascular fluid and proteins into the alveoli, while inflammatory cells, particularly neutrophils, migrated into the lungs under the influence of inflammatory factors such as interleukin-1 $\beta$  (IL-1 $\beta$ ) and tumor necrosis factor- $\alpha$  (TNF- $\alpha$ ). However, treatment with TMP reduced the protein concentration and total white blood cell count in the BALF, particularly neutrophils. Additionally, this experiment assessed the W/D of lung tissue. The results demonstrated that LPS, as an endotoxin, activates immune cells and stimulates the production of inflammatory mediators, thereby increasing vascular permeability and facilitating the movement of plasma components and leukocytes into the alveolar space and cavity. Consequently, the weight of lung tissue increased, along with the W/D. In contrast, pretreatment with TMP decreased the W/D of lung tissue, reduced vascular permeability, and mitigated pulmonary edema, which is in line with the findings from the Hep group.

LPS activates the host's immune response by binding to TLR4 and promoting the release of HMGB1 from the nucleus into the extracellular space. Extracellular HMGB1 can further bind to TLR4, thereby enhancing the inflammatory effects of LPS and resulting in a more intense inflammatory reaction. TMP has been shown to inhibit both pyroptosis and apoptosis in AM, which subsequently reduces the transcription and secretion of inflammatory factors such as LPS-induced IL-1 $\beta$ , IL-18, and TNF- $\alpha$  (23). TLR4 is primarily localized in AM and lung epithelial cells (24), while HMGB1 is also widely distributed throughout lung tissue. The release of HMGB1 in the lungs aggravates the activation of the TLR4/NF- $\kappa$ B signaling pathway, which can induce a pulmonary inflammatory response. This response subsequently damages alveolar epithelial cells and endothelial cells, increases vascular permeability, and leads to alveolar exudation and edema (25). The transcription factor NF- $\kappa$ B is activated in response to various signals, triggering the expression of inflammatory

factors such as IL-1 $\beta$  and TNF- $\alpha$ . Additionally, it promotes the transcription of the *HMGB1* gene, resulting in increased expression and release of HMGB1 (24,26,27). Once released into the extracellular space, HMGB1 binds to TLR4, further activating TLR4 and its downstream pathways, which creates a positive feedback loop that exacerbates the inflammatory response. Western blot results indicate that LPS enhances HMGB1 expression, which in turn activates TLR4, leading to an increase in TLR4 expression and subsequent activation of downstream NF- $\kappa$ B-p65. This cascade results in elevated levels of p-p65, facilitating nuclear translocation and promoting the release of various inflammatory factors, including HMGB1. This sequence of events ultimately contributes to the formation of positive feedback and further aggravation of inflammation, demonstrating that LPS effectively induces the inflammatory response in ALI. Conversely, TMP demonstrated a protective effect in this model. Previous research from our group showed that TMP inhibits the expression of the pro-inflammatory cytokines TNF- $\alpha$  and IL-1 $\beta$  in serum, suggesting a broader systemic anti-inflammatory effect (19). This observation is consistent with multiple studies demonstrating TMP's influence on the TLR4 signaling pathway and its downstream effects (23,28-31). Specifically, TMP counteracts the LPS-induced upregulation of CD14, a crucial accessory molecule in the TLR4 pathway responsible for LPS recognition and transfer to the TLR4/MD-2 complex (31,32). This suggests that TMP may indirectly inhibit TLR4 signaling through its modulation of CD14. In the present study, the observed reductions in HMGB1, TLR4, and p-p65 protein expression support the hypothesis that TMP ameliorates LPS-induced ALI through the HMGB1/TLR4/NF- $\kappa$ B signaling pathway (Figure 7). However, whether this effect involves a direct interaction with the TLR4 receptor remains a subject for future investigation.

In summary, TMP has the potential to mitigate the increased pulmonary vascular permeability and pulmonary edema associated with the inflammatory response in ALI mice, demonstrating a protective effect on these subjects. The activation of the HMGB1/TLR4/NF- $\kappa$ B pathway induced by LPS can trigger an inflammatory response in the lungs, leading to a cascade effect that may play a crucial role in the rapid onset and exacerbation of ALI symptoms. TMP appears to attenuate this cascade effect of lung inflammation by inhibiting the HMGB1/TLR4/NF- $\kappa$ B pathway, thereby alleviating LPS-induced ALI. This provides a significant experimental and theoretical foundation for the clinical

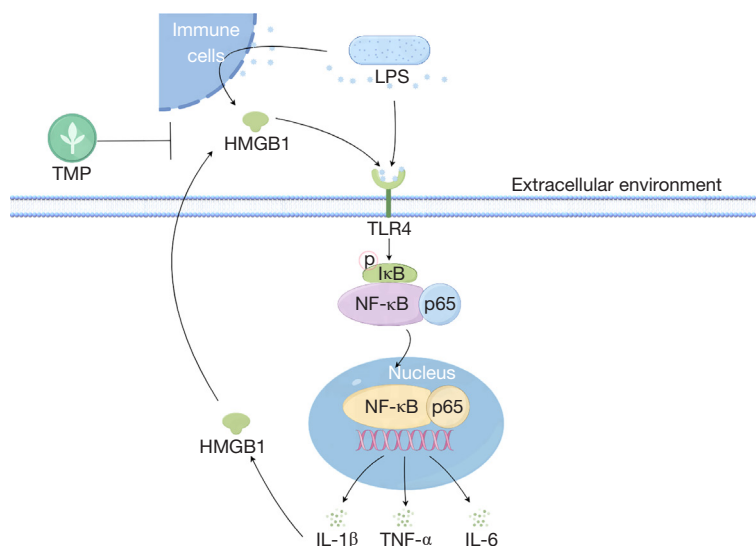


**Figure 7** HMGB1/TLR4/NF- $\kappa$ B signaling pathway activation induced by LPS, and the protective mechanism of TMP. HMGB1, high mobility group box 1; IL, interleukin; LPS, lipopolysaccharide; NF- $\kappa$ B, nuclear factor kappa-B; TLR4, Toll-like receptor 4; TNF- $\alpha$ , tumor necrosis factor- $\alpha$ ; TMP, tetramethylpyrazine.

application of TMP in treatment.

However, there are some limitations in this study. Initially, while the method of quantitative nebulization of LPS in mice demonstrates significant advantages in efficacy, it imposes technical demands on the experimenters and necessitates the collaboration of two individuals. Consequently, a period of technical training is imperative. Additionally, we utilized a single-dose treatment medication that has proven effective against ALI, showing a notable reduction in proteins associated with the HMGB1/TLR4/NF- $\kappa$ B pathway. Yet, the precise impact of alternative dosages on this pathway remains to be elucidated, presenting an opportunity for further investigation in future studies.

## Conclusions

This study indicates that TMP can alleviate systemic inflammatory responses induced by LPS in mice with ALI and may exert its effects through the HMGB1/TLR4/NF- $\kappa$ B signaling pathway.

## Acknowledgments

None.

## Footnote

**Reporting Checklist:** The authors have completed the ARRIVE reporting checklist. Available at <https://jtd.amegroups.com/article/view/10.21037/jtd-24-1561/rc>

**Data Sharing Statement:** Available at <https://jtd.amegroups.com/article/view/10.21037/jtd-24-1561/dss>

**Peer Review File:** Available at <https://jtd.amegroups.com/article/view/10.21037/jtd-24-1561/prf>

**Funding:** This study was supported by the National Natural Science Foundation of China (No. 81673791) and Changzhou University High-Level Talents Project (No. ZMF22020010).

**Conflicts of Interest:** All authors have completed the ICMJE uniform disclosure form (available at <https://jtd.amegroups.com/article/view/10.21037/jtd-24-1561/coif>). The authors have no conflicts of interest to declare.

**Ethical Statement:** The authors are accountable for all aspects of the work in ensuring that questions related to the accuracy or integrity of any part of the work

are appropriately investigated and resolved. All animal experiments were performed under a project license (No. 20240308049) granted by the Biomedical Research Ethics Committee of Changzhou University, in compliance with Chinese national guidelines for the care and use of animals.

**Open Access Statement:** This is an Open Access article distributed in accordance with the Creative Commons Attribution-NonCommercial-NoDerivs 4.0 International License (CC BY-NC-ND 4.0), which permits the non-commercial replication and distribution of the article with the strict proviso that no changes or edits are made and the original work is properly cited (including links to both the formal publication through the relevant DOI and the license). See: <https://creativecommons.org/licenses/by-nc-nd/4.0/>.

## References

1. Sweeney RM, McAuley DF. Acute respiratory distress syndrome. *Lancet* 2016;388:2416-30.
2. Yin S, Ding M, Fan L, et al. Inhibition of Inflammation and Regulation of AQP/ENaCs/Na(+)-K(+)-ATPase Mediated Alveolar Fluid Transport by Total Flavonoids Extracted From *Nervilia fordii* in Lipopolysaccharide-induced Acute Lung Injury. *Front Pharmacol* 2021;12:603863.
3. Li L, Zhou B, Xu H, et al. Zinc-loaded black phosphorus multifunctional nanodelivery system combined with photothermal therapy have the potential to treat prostate cancer patients infected with COVID-19. *Front Endocrinol (Lausanne)* 2022;13:872411.
4. Yu H, Lin L, Zhang Z, et al. Targeting NF- $\kappa$ B pathway for the therapy of diseases: mechanism and clinical study. *Signal Transduct Target Ther* 2020;5:209.
5. Zuo W, Tian F, Ke J, et al. Mechanisms and Research Progress of Traditional Chinese Medicine Regulating NF- $\kappa$ B in the Treatment of Acute Lung Injury/Acute Respiratory Distress Syndrome. *Chinese Medicine and Natural Products* 2024;4:e93-e105.
6. Guo M, Liu Y, Shi D. Cardiovascular Actions and Therapeutic Potential of Tetramethylpyrazine (Active Component Isolated from *Rhizoma Chuanxiong*): Roles and Mechanisms. *Biomed Res Int* 2016;2016:2430329.
7. Zhang Y, Ma C, He L, et al. Tetramethylpyrazine Protects Endothelial Injury and Antithrombosis via Antioxidant and Antiapoptosis in HUVECs and Zebrafish. *Oxid Med Cell Longev* 2022;2022:2232365.
8. Zheng ZX, Peng XM, Xi L, et al. Protective effects of perfluorocarbon combined with ligustrazine against lung ischemia-reperfusion injury in rats. *Nan Fang Yi Ke Da Xue Xue Bao* 2016;36:250-4.
9. Rice TW, Wheeler AP, Bernard GR, et al. Comparison of the SpO<sub>2</sub>/FIO<sub>2</sub> ratio and the PaO<sub>2</sub>/FIO<sub>2</sub> ratio in patients with acute lung injury or ARDS. *Chest* 2007;132:410-7.
10. Yang J, Chen Y, Jiang K, et al. MicroRNA-106a provides negative feedback regulation in lipopolysaccharide-induced inflammation by targeting TLR4. *Int J Biol Sci* 2019;15:2308-19.
11. Tan W, Zhang C, Liu J, et al. Regulatory T-cells promote pulmonary repair by modulating T helper cell immune responses in lipopolysaccharide-induced acute respiratory distress syndrome. *Immunology* 2019;157:151-62.
12. Zhang F, Li Y, Xi Y, et al. Qinbaohong Zhike Oral Liquid Attenuates LPS-Induced Acute Lung Injury in Immature Rats by Inhibiting OLFM4. *Oxid Med Cell Longev* 2022;2022:7272371.
13. Shi Y, Liu T, Nieman DC, et al. Aerobic Exercise Attenuates Acute Lung Injury Through NET Inhibition. *Front Immunol* 2020;11:409.
14. Yang B, Li H, Qiao Y, et al. Tetramethylpyrazine Attenuates the Endotheliotoxicity and the Mitochondrial Dysfunction by Doxorubicin via 14-3-3 $\gamma$ /Bcl-2. *Oxid Med Cell Longev* 2019;2019:5820415.
15. Chen Q, Liu C, Gu Q, et al. An injectable thermosensitive hydrogel encapsulating tetramethylpyrazine nanocrystals alleviates angiogenesis and apoptosis in a choroidal neovascularization mouse model. *Applied Materials Today* 2023;33:101867.
16. Jiang Y, Yan Q, Liu CX, et al. Insights into potential mechanisms of asthma patients with COVID-19: A study based on the gene expression profiling of bronchoalveolar lavage fluid. *Comput Biol Med* 2022;146:105601.
17. Zhou L, Chen J, Mu G, et al. Heparin-binding protein (HBP) worsens the severity of pancreatic necrosis via up-regulated M1 macrophages activation in acute pancreatitis mouse models. *Bioengineered* 2021;12:11978-86.
18. Boyle AJ, Mac Sweeney R, McAuley DF. Pharmacological treatments in ARDS; a state-of-the-art update. *BMC Med* 2013;11:166.
19. Min S, Tao W, Ding D, et al. Tetramethylpyrazine ameliorates acute lung injury by regulating the Rac1/LIMK1 signaling pathway. *Front Pharmacol* 2022;13:1005014.
20. Tao W, Min S, Chen G, et al. Tetramethylpyrazine ameliorates LPS-induced acute lung injury via the miR-369-3p/DSTN axis. *Sci Rep* 2024;14:20006.

21. Asai A, Tsuchimoto Y, Ohama H, et al. CD34+CD10+CD19- cells in patients with unhealthy alcohol use stimulate the M2b monocyte polarization. *Cells* 2022;11:2703.
22. Hu C, Li J, Tan Y, et al. Tanreqing Injection Attenuates Macrophage Activation and the Inflammatory Response via the lncRNA-SNHG1/HMGB1 Axis in Lipopolysaccharide-Induced Acute Lung Injury. *Front Immunol* 2022;13:820718.
23. Jiang R, Xu J, Zhang Y, et al. Ligustrazine alleviate acute lung injury through suppressing pyroptosis and apoptosis of alveolar macrophages. *Front Pharmacol* 2021;12:680512.
24. Chen R, Kang R, Tang D. The mechanism of HMGB1 secretion and release. *Exp Mol Med* 2022;54:91-102.
25. Lu YC, Yeh WC, Ohashi PS. LPS/TLR4 signal transduction pathway. *Cytokine* 2008;42:145-51.
26. Fu Y, Xiang Y, Wang Y, et al. The STAT1/HMGB1/NF- $\kappa$ B pathway in chronic inflammation and kidney injury after cisplatin exposure. *Theranostics* 2023;13:2757-73.
27. Liang WJ, Yang HW, Liu HN, et al. HMGB1 upregulates NF- $\kappa$ B by inhibiting IKB- $\alpha$  and associates with diabetic retinopathy. *Life Sci* 2020;241:117146.
28. Lin J, Wang Q, Zhou S, et al. Tetramethylpyrazine: A review on its mechanisms and functions. *Biomed Pharmacother* 2022;150:113005.
29. Lei J, Xiang P, Zeng S, et al. Tetramethylpyrazine Alleviates Endothelial Glycocalyx Degradation and Promotes Glycocalyx Restoration via TLR4/NF- $\kappa$ B/HPSE1 Signaling Pathway During Inflammation. *Front Pharmacol* 2021;12:791841.
30. Jiang T, Wang CY, Chen Y. Tetramethylpyrazine inhibits keratitis and neovascularization induced by corneal alkali burn by suppressing the TLR4/NF- $\kappa$ B pathway activation and NLRP1/NLRP3 inflammasomes in rats. *Exp Eye Res* 2023. [Epub ahead of print]. doi: 10.1016/j.exer.2023.109704.
31. Han X, Chen X, Chen S, et al. Tetramethylpyrazine attenuates endotoxin-induced retinal inflammation by inhibiting microglial activation via the TLR4/NF- $\kappa$ B signalling pathway. *Biomed Pharmacother* 2020;128:110273.
32. Ciesielska A, Matyjek M, Kwiatkowska K. TLR4 and CD14 trafficking and its influence on LPS-induced pro-inflammatory signaling. *Cell Mol Life Sci* 2021;78:1233-61.

**Cite this article as:** He X, Chen GF, Tao WT, Huang XJ, Lin Y, Sun J, Li Y. Tetramethylpyrazine mitigates lipopolysaccharide-induced acute lung injury by inhibiting the HMGB1/TLR4/NF- $\kappa$ B signaling pathway in mice. *J Thorac Dis* 2025;17(3):1605-1616. doi: 10.21037/jtd-24-1561